Analysis and simulation of the basic structures
of active EMI filters

Marian Pasko, Marek Szymczak
Silesian University of Technology
44-100 Gliwice, ul. Akademicka 10, e-mail: Marian.Pasko@polsl.pl,
Marek Szymczak@polsl.pl

The main goals of this paper are an analysis and a simulation of selected basic structures of active EMI filters. The first part contains a presentation of selected structures of active filters, along with categorization by their properties in the field of detection and compensation of EMI noise and by the kind of feedback. Each structure's description is accompanied by an analytical discussion of their properties such as insertion loss (*IL*) and the impedance increase (ΔZ_n). The second part contains results of simulations of the presented structures, with the aim being a comparison of their characteristics and determining proper operation conditions.

KEYWORDS: active filters, conducted noise, electromagnetic compatibility, EMI filters

1. Introduction

The first publications about the active EMI filters were presented in mid '80's [10, 11] but the development of new converters that operate at high frequencies increased their significance [3, 8, 10]. The high level of EMI noise generated by modern converters [1] renewed interest in this subject [4, 13]. The systems that are most commonly used for attenuation of the conducted ripple are passive filters, made up mainly of RLC components, but their drawback are size and cost [15]. For many years research was being conducted on the use of active filters for suppressing EMI by replacing passive filters or improving their performance [2, 5, 6, 9]. Significant progress in the technology that allowed construction of light converters operating at high frequencies, paradoxically led to the fact that the weight of EMI filters can be greater than the weight of the inverter [7, 12].

The goal of an active filter is detecting and rejecting noise generated by a source (receiver) so that it does not propagate to the mains (Figure 1). There are several different filter configurations which differ in the type of feedback and a way of detecting and cancelling noise. Due to the type of feedback the active filters can be divided into two groups: feedback type and feedforward type.
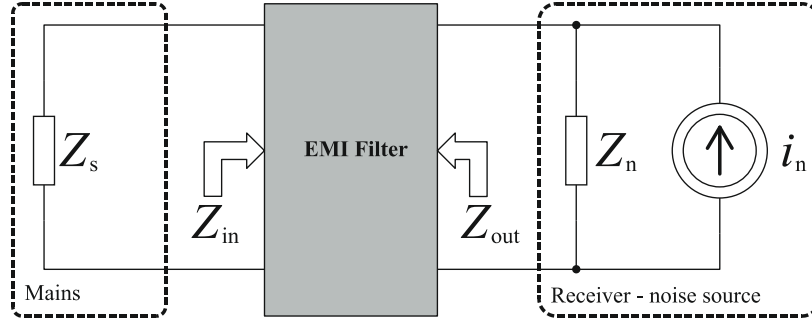
Fig. 1. Equivalent circuit with EMI filter

The ratio of reduction of the EMI noise is an insertion loss *IL*, defined as (1) the ratio of a RMS voltage on the receiver terminals without any filter and the RMS voltage on these terminals with a filter:

$$|IL| = \frac{\left|U_s^0\right|}{\left|U_s\right|}$$

(1)

and in the logarithmic scale (2):

$$|IL_{dB}| = 20log\frac{\left|U_s^0\right|}{\left|U_s\right|}$$

(2)

where: U_s^0 - the RMS voltage on the receiver terminals without any filter, U_s - the RMS voltage on the receiver terminals with a filter.

The second parameter specifies a filter property known as impedance increase ΔZ_n [14]. This parameter represents the difference between the receiver impedance with a filter Z_{in}, and the pure receiver impedance Z_n (3):

$$\Delta Z_n = Z_{in} - Z_n$$

(3)

2. Structures of the active EMI filters

This chapter discusses derivation of the basic parameters of the active EMI filters that will be used in next chapter for simulations.

2.1. Feedback type active filters

The main tasks of the feedback filter are detecting noise at the noise source (receiver) and generating a compensating signal so that it suppresses the ripples generated by the source (closed loop). In Figure 2 there are shown four basic structures of the feedback type active filters [11], and the type number proposed

them in [14]. These types differ from each other a way of detecting and cancelling noise .
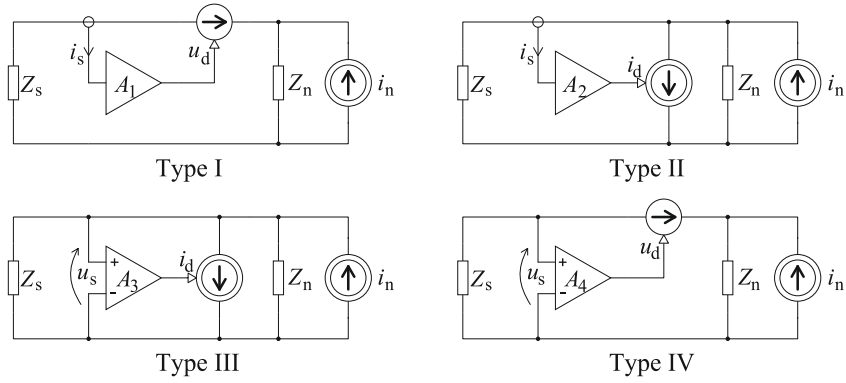

Fig. 2. Feedback type active filters[11]

Type I: current detecting and voltage compensating filters

Insertion loss of type I filter may be determined by assuming that the voltage controlled current source (a current that flows through it) is an impedance proportional to the filter gain A_1. In Figure 3 a circuit for determining the IL_1 (7) has been presented (Figure 3a - measurement of voltage at the receiver with a filter and 3b - without a filter).
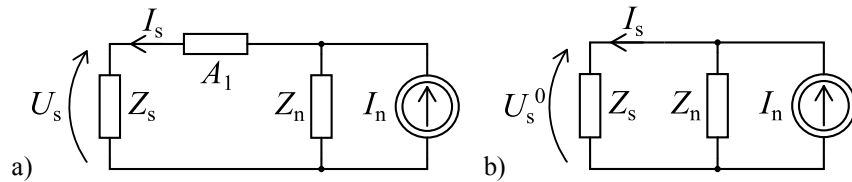

Fig. 3. Equivalent circuit to determine the IL_1: a) receiver with a filter,
b) receiver without any filter

$$U_S^0 = I_n \cdot \frac{Z_n \cdot Z_s}{Z_n + Z_s} \tag{4}$$

$$I_S = I_n \cdot \frac{Z_n}{Z_n + Z_s + A_1} \tag{5}$$

$$U_S = I_S \cdot Z_S = I_n \cdot \frac{Z_n \cdot Z_s}{Z_n + Z_s + A_1} \tag{6}$$

$$IL_1 = \frac{U_s^0}{U_s} = \frac{I_n \cdot \dfrac{Z_n \cdot Z_s}{Z_n + Z_s}}{I_n \cdot \dfrac{Z_n \cdot Z_s}{Z_n + Z_s + A_1}} = \frac{Z_n + Z_s + A_1}{Z_n + Z_s} = 1 + \frac{A_1}{Z_n + Z_s} \tag{7}$$
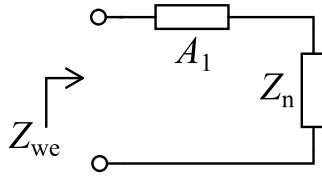

Fig. 4. Equivalent circuit to determine the impedance increase ΔZ_{n1}

To determine the impedance increase ΔZ_{n1} (8) the same circuit as in the insertion loss case can be used, where controlled current source is impedance of A_1 value (Figure 4).

$$\Delta Z_{n1} = Z_{we} - Z_n = A_1 + Z_n - Z_n = A_1 \tag{8}$$

Type II: current detecting and current compensating filters

For determining the insertion loss IL_2 (11) of type II filters, a schematics shown in Figure 5 can be used (U_s^0 has the same meaning as in type I filters).
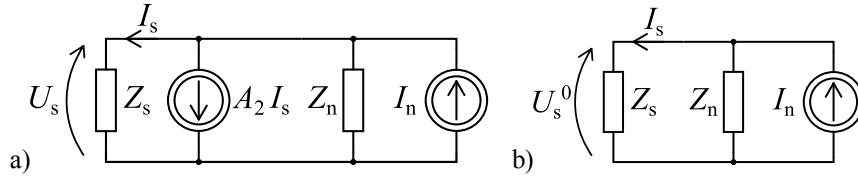

Fig. 5. Equivalent circuit to determine the IL_2: a) receiver with a filter,
b) receiver without any filter

$$I_S = \frac{Z_n}{Z_n + Z_s}\left(I_n - A_2 \cdot I_S\right) = \frac{I_n \cdot Z_n}{Z_n + Z_s + A_2 \cdot Z_n} \tag{9}$$

$$U_S = I_S \cdot Z_S = \frac{I_n \cdot Z_n \cdot Z_s}{Z_n + Z_s + A_2 \cdot Z_n} \tag{10}$$

$$IL_2 = \frac{U_s^0}{U_s} = \frac{I_n \cdot \dfrac{Z_n \cdot Z_s}{Z_n + Z_s}}{I_n \cdot \dfrac{Z_n \cdot Z_s}{Z_n + Z_s + A_2 \cdot Z_n}} = \frac{Z_n + Z_s + A_2 \cdot Z_n}{Z_n + Z_s} = 1 + \frac{A_2 \cdot Z_n}{Z_n + Z_s} \tag{11}$$

91

To determine the impedance increase ΔZ_{n2} (14) the schematics shown in Figure 6 can be used. Gain A_2 in this figure is negative because the current I_s is marked in the opposite direction in regard to Figure 5a.
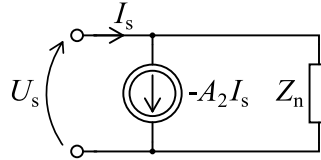

Fig. 6. Equivalent circuit to determine the impedance increase ΔZ_{n2}

$$U_S = \left(I_S + A_2 \cdot I_S\right)\cdot Z_n = I_S \cdot \left(Z_n + A_2 \cdot Z_n\right) \qquad (12)$$

$$Z_{we} = \frac{U_S}{I_S} = Z_n + A_2 \cdot Z_n \qquad (13)$$

$$\Delta Z_{n2} = Z_{we} - Z_n = Z_n + A_2 \cdot Z_n - Z_n = A_2 \cdot Z_n \qquad (14)$$

Type III: voltage detecting and current compensating filters

The insertion loss of type III filter can be determined by using an analogy to type I filters and replacing the controlled current source with an admittance of value A_3. Figure 7a presents a schematics for determining IL_3 (15).
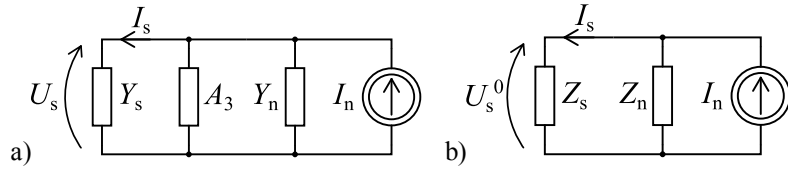

Fig. 7. Equivalent circuit to determine the IL_3: a) receiver with a filter, b) receiver without any filter

$$IL_3 = \frac{U_S^0}{U_S} = \frac{\dfrac{I_n}{Y_n + Y_s}}{\dfrac{I_n}{Y_n + Y_s + A_3}} = \frac{Y_n + Y_s + A_3}{Y_n + Y_s} = 1 + \frac{A_3}{Y_n + Y_s} \qquad (15)$$

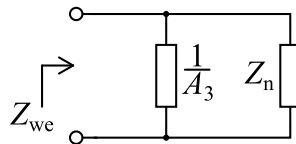Figure 8 shows a circuit for determining the impedance increase ΔZ_{n3} (16).

Fig. 8. Equivalent circuit to determine the impedance increase ΔZ_{n3}

$$\Delta Z_{n3} = Z_{we} - Z_n = \frac{Z_n}{1 + Z_n \cdot A_3} - Z_n = \frac{Z_n}{1 + Z_n \cdot A_3} - \frac{Z_n + Z_n^2 \cdot A_3}{1 + Z_n \cdot A_3} = -\frac{Z_n^2 \cdot A_3}{1 + Z_n \cdot A_3}$$

$$(16)$$

Type IV: voltage detecting and voltage compensating filters

To simplify the calculation of the insertion loss IL_4 (17) for type IV filters, the noise source model has been changed from a current to a voltage one. Such modified circuit diagram has been shown in Figure 9 and can be considered an analogy to the filter type II.
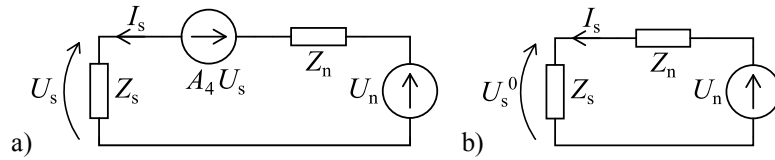

Fig. 9. Equivalent circuit to determine the IL_4: a) receiver with a filter,
b) receiver without any filter

$$IL_4 = \frac{U_s^0}{U_s} = \frac{U_n \cdot \dfrac{Z_s}{Z_n + Z_s}}{U_n \cdot \dfrac{Z_s}{Z_n + Z_s + A_4}} = \frac{Z_n + Z_s + A_4 \cdot Z_s}{Z_n + Z_s} = 1 + \frac{A_4 \cdot Z_s}{Z_n + Z_s} \qquad (17)$$

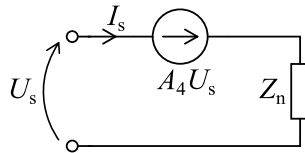Figure 10 shows a circuit for determine the impedance increase ΔZ_{n4} (18).

Fig. 10. Equivalent circuit to determine the impedance increase ΔZ_{n4}

$$\Delta Z_{n4} = Z_{we} - Z_n = \frac{Z_n}{1 + A_4} - Z_n = \frac{Z_n}{1 + A_4} - \frac{Z_n + A_4 \cdot Z_n}{1 + A_4} = -\frac{A_4 \cdot Z_n}{1 + A_4} \qquad (18)$$

2.2. Feedforward type active filters

The feedforward type active filters generate a signal opposite to the noise generated by the receiver, so that the two signals cancel out each other. The effectiveness of the attenuation is greater when the filter gain is close to unity.

In contrast to feedback type filters, only two configurations can be singled out, both of which has been illustrated in Figure 11 with the type number proposed them in [14].
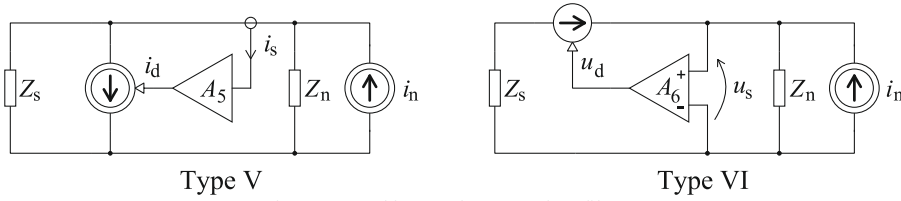

Fig. 11. Feedforward type active filters

Type V: current detecting and current compensating filters

To analyze the insertion loss IL_5 (22) of a type V filter a circuit shown in Figure 12 has been proposed. In the analysis a current I_x, which represents the noise current between the filter and the receiver (the source of noise), has been added.
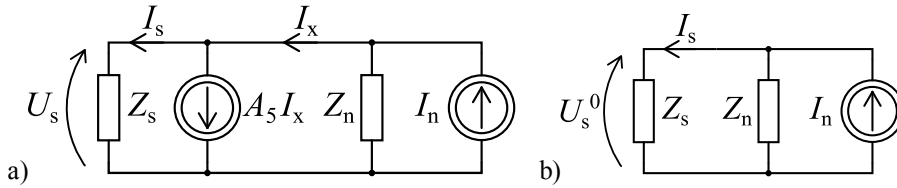

Fig. 12. Equivalent circuit to determine the IL_5: a) receiver with a filter,
b) receiver without any filter

$$I_x = I_S + A_5 \cdot I_x = \frac{I_S}{1 - A_5} \tag{19}$$

$$I_S = \frac{Z_n}{Z_n + Z_S} \cdot (I_n - A_5 \cdot I_x) = I_n \cdot \frac{Z_n}{Z_n + Z_S + \dfrac{A_5 \cdot Z_n}{1 - A_5}} \tag{20}$$

$$U_S = I_S \cdot Z_S = I_n \cdot \frac{Z_n \cdot Z_S}{Z_n + Z_S + \dfrac{A_5 \cdot Z_n}{1 - A_5}} \tag{21}$$

$$IL_5 = \frac{U_S^0}{U_S} = \frac{I_n \cdot \dfrac{Z_n \cdot Z_S}{Z_n + Z_S}}{I_n \cdot \dfrac{Z_n \cdot Z_S}{Z_n + Z_S + \dfrac{A_5 \cdot Z_n}{1 - A_5}}} = \frac{Z_n + Z_S + \dfrac{A_5 \cdot Z_n}{1 - A_5}}{Z_n + Z_S} = \frac{1}{1 - A_5} \cdot \left(1 - \frac{Z_S \cdot A_5}{Z_n + Z_S}\right)$$

$$\tag{22}$$

94

Figure 13 shows a circuit for determining the impedance increase ΔZ_{n5} (23).
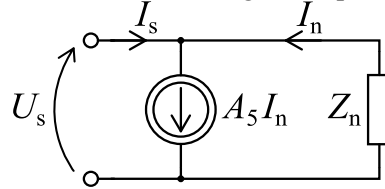

Fig. 13. Equivalent circuit to determine the impedance increase ΔZ_{n5}

$$\Delta Z_{n5} = Z_{we} - Z_n = \frac{Z_n}{1 - A_5} - Z_n = \frac{Z_n}{1 - A_5} - \frac{Z_n - Z_n \cdot A_5}{1 - A_5} = \frac{Z_n \cdot A_5}{1 - A_5} \quad (23)$$

Type VI: voltage detecting and voltage compensating filters

The difference in analysis of the type VI filter from the previous type consists of replacing the noise source model from a current to a voltage one. A circuit for determining the IL_6 (24) has been shown in Figure 14.
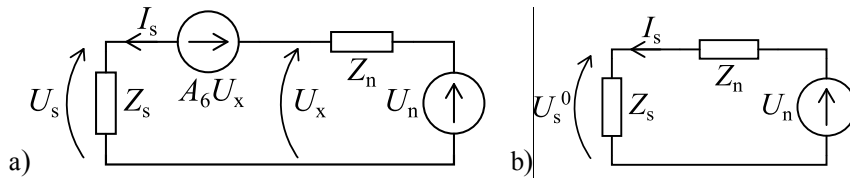

Fig. 14. Equivalent circuit to determine the IL_6: a) receiver with a filter, b) receiver without any filter

$$IL_6 = \frac{U_s^0}{U_s} = \frac{Z_s}{Z_n + Z_s} \cdot \frac{Z_n + Z_s + \frac{Z_s \cdot A_6}{1 - A_6}}{Z_s} = \frac{Z_n + Z_s + \frac{Z_s \cdot A_6}{1 - A_6}}{Z_n + Z_s} = \frac{1}{1 - A_6} \cdot \left(1 - \frac{Z_n \cdot A_6}{Z_n + Z_s}\right)$$

$$(24)$$

Figure 15 shows a circuit for determining the impedance increase ΔZ_{n6} (25).
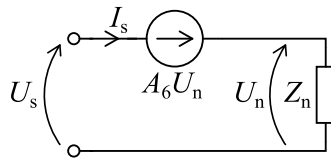

Fig. 15. Equivalent circuit to determine the impedance increase ΔZ_{n6}

$$\Delta Z_{n6} = Z_{we} - Z_n = Z_n - A_6 \cdot Z_n - Z_n = -A_6 \cdot Z_n \quad (25)$$

95

3. Simulations of active filters

This chapter discusses the results of simulation analysis of previously obtained equations to investigate their behavior, depending on changes in individual parameters such as the impedance module of noise sources $|Z_n|$ and filter gain module $|A|$.

3.1. Simulations of the feedback type filters

In the previous chapter the basic parameters of active feedback filters have been presented. Their summary can be found in Table 1: I - current detecting and voltage compensating filters, II - current detecting and current compensating filters, III - voltage detecting and current compensating filters, IV - voltage detecting and voltage compensating filters.

Figure 16 shows changes in the insertion loss module $|IL|$, depending on the ratio of noise source impedance module ($|Z_n|$) and the network impedance module ($|Z_s|$) for a constant gain module $|A|$ and for a different types of filters.

Table 1. Summary of basic parameters of the feedback filters

Type	Filter gain	Insertion loss	Impedance increase
I	$A_1 = \dfrac{U_d}{I_s}$	$IL_1 = 1 + \dfrac{A_1}{Z_n + Z_s}$	$\Delta Z_{n1} = A_1$
II	$A_2 = \dfrac{I_d}{I_s}$	$IL_2 = 1 + \dfrac{A_2 \cdot Z_n}{Z_n + Z_s}$	$\Delta Z_{n2} = A_2 \cdot Z_n$
III	$A_3 = \dfrac{I_d}{U_s}$	$IL_3 = 1 + \dfrac{A_3}{Y_n + Y_s}$	$\Delta Z_{n3} = -\dfrac{Z_n^{\,2} \cdot A_3}{1 + Z_n \cdot A_3}$
IV	$A_4 = \dfrac{U_d}{U_s}$	$IL_4 = 1 + \dfrac{A_4 \cdot Z_s}{Z_n + Z_s}$	$\Delta Z_{n4} = -\dfrac{A_4 \cdot Z_n}{1 + A_4}$

Analyzing the Figure 16, it can be concluded that for the correct operation of the filter type I and IV, which perform voltage compensation of noise, the noise source impedance modulus $|Z_n|$ is required to be smaller than the mains impedance modulus $|Z_s|$. In contrast, for Type II and III, the noise source impedance module need to be much larger than the mains impedance module. The gain module of the filters is the same for all types and equals $|A| = 100$.

Figure 17 shows diagrams of changes of the insertion loss module $|IL_{dB}|$ in regard to the filter gain module $|A|$ for various values of noise source impedance module $|Z_n|$. From these graphs the behavior of filters with different values of the source impedance module can be evaluated. The common denominator for

obtaining high effectiveness of noise suppression is the largest possible value of the filter gain module.
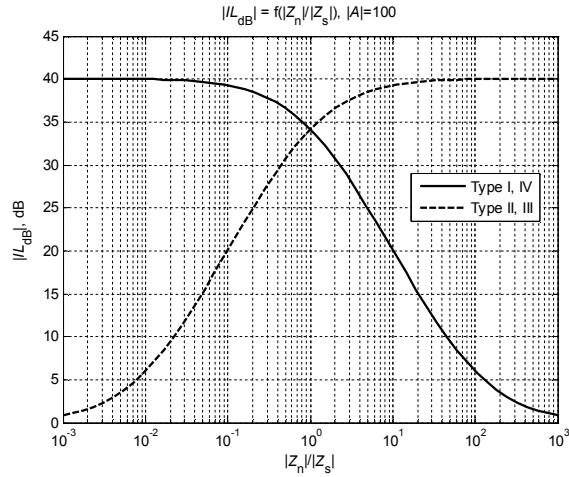

Fig. 16. Changes in the insertion loss module depending on the ratio of noise source impedance module and the network impedance module for a different filter types
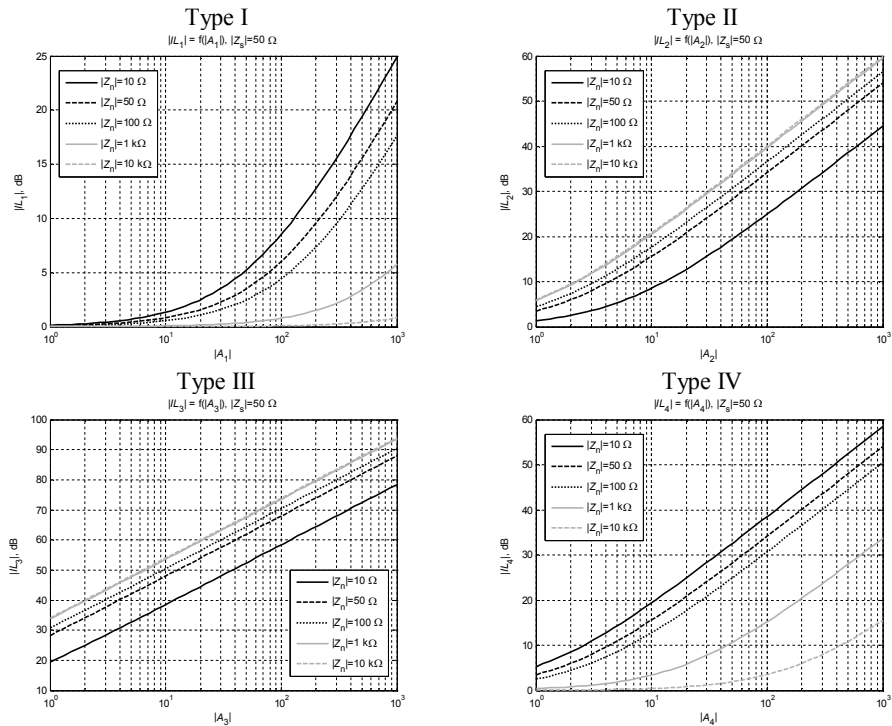

Fig. 17. Changes in the insertion loss module depending on change the gain module for a different filter types

By analyzing impedance increase module $|\Delta Z_n|$ as shown in Table 1 it can be seen that for current detecting filters (type I and II) it has a positive value, but for filters that detects voltage (type III and IV) it is negative.

3.2. Simulations of the feedforward type filters

Table 2 summarize the basic parameters of the feedforward filters. Unlike the feedback filter there only two configurations are possible: V - current detecting and current compensating filters, VI - voltage detecting and voltage compensating filters.

Table 2. Summary of basic parameters of the feedforward filters

Type	Filter gain	Insertion loss	Impedance increase
V	$A_5 = \dfrac{I_s}{I_d}$	$IL_5 = \dfrac{1}{1 - A_5} \cdot \left(1 - \dfrac{Z_s \cdot A_5}{Z_n + Z_s} \right)$	$\Delta Z_{n5} = \dfrac{Z_n \cdot A_5}{1 - A_5}$
VI	$A_6 = \dfrac{U_s}{U_d}$	$IL_6 = \dfrac{1}{1 - A_6} \cdot \left(1 - \dfrac{Z_n \cdot A_6}{Z_n + Z_s} \right)$	$\Delta Z_{n6} = -A_6 \cdot Z_n$

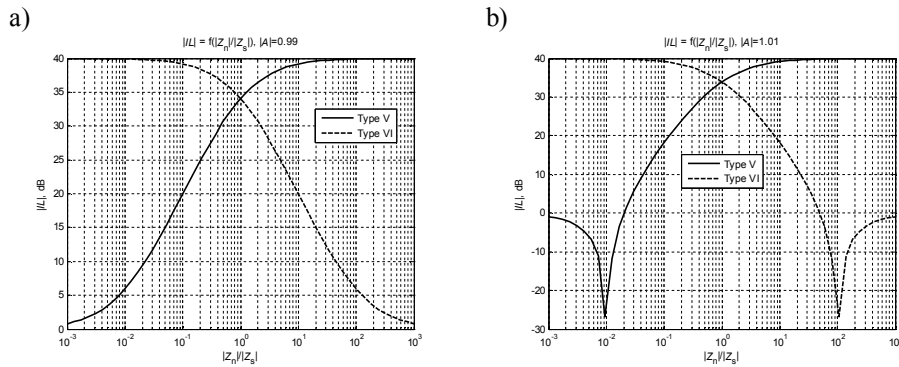a)   b)

Fig. 18. Changes in the insertion loss module depending on the ratio of noise source impedance module and the network impedance module for a different filter gain: a) $|A| = 0,99$; b) $|A| = 1,01$

In the graphs in Figure 18 it can be seen that, as in the filters with feedback, for the voltage detecting filter (type V) the source impedance module is required to be much larger than the mains impedance module. Similarly for the filter VI, for effective suppression of noise high source impedance module is required. In contrast to the feedback filter, for obtaining a large damping factor the gain of the filters should be close to unity. The simulation assumed value of $A \neq 1$, because when gain is equal to one, the equations of these filters do not make sense (division by 0). Assuming $|Z_n| \gg |Z_s|$ for the filter V, the insertion loss

equation can be simplified to (26) and for the filter VI, assuming $|Z_n| << |Z_s|$, the insertion loss can be simplified to (27).

$$|IL_5| \cong \frac{1}{1-|A_5|}, \text{dla} \, |Z_n| >> |Z_s| \qquad (26)$$

$$|IL_6| \cong \frac{1}{1-|A_6|}, dla \, |Z_n| << |Z_s| \qquad (27)$$

Figure 19 shows changes in the insertion loss module $|IL_{dB}|$ depending on the filter gain module for different values of the noise source impedance modulus $|Z_n|$. This gain is changed within a narrow range (0.1 to 10) because the larger value of its changes do not make sense. As mentioned, in the feedforward filters, the gain is required to be close to unity, and diagrams of Figure 19 show the sensitivity of the filter to its changes for different values of impedance modulus $|Z_n|$.
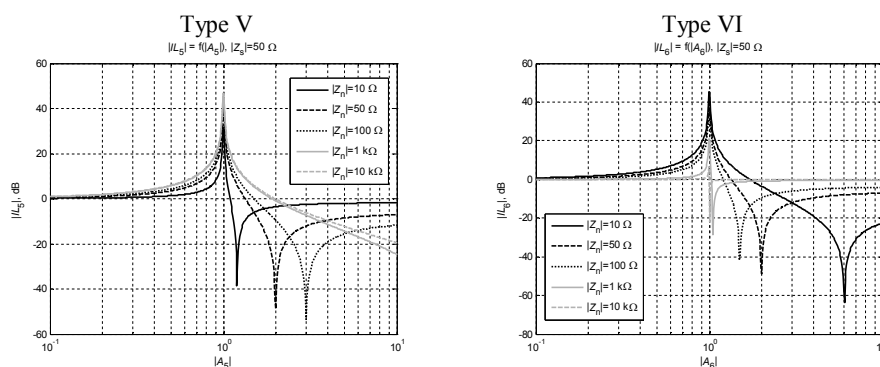

Fig. 19. Changes in the insertion loss module depending on change the gain module
for a different filter types

Assessing changes of impedance increase modules shown in Table 2, it can be seen that it is positive for the filter with current detection, and negative for the filter that detect voltage.

4. Selection of a filter type

Analyzing the simulation results, it can be noticed that each of these filter types is adequate for reduction of a specific type of noise and that active filters affect the nature of the impedance of the receiver at the mains side.

Type I, IV and VI filters that compensate voltage are adequate for systems in which the noise source can be modeled by a voltage source (where $|Z_n| \to 0$). In contrast to that, the current compensating filters are a good option in systems where the noise source can be modeled by a current source (where $|Z_n| \to \infty$). In a type II, III and V filters a method of reducing noise is to redirect the current

flow back to the receiver. As a result, current does not go to the mains, but comes back to the noise source. Similarly, in filters of type I, IV and VI, where the voltage is compensated, the system blocks the noise flow to the mains by trying to generate a voltage opposite to the noise voltage. This situation corresponds to a break in the circuit [13].

Analyzing the impedance increase module, it can be notice that filters of type I, II and V increase the impedance module of the receiver, and filters of type III, IV and VI reduce it. It is related to the noise detection method. When designing a filter, it should be ensured that operation of the filter begins with the frequency much greater than the mains frequency, which is particularly important for filter types III, IV and VI, which reduce the impedance of the receiver. Without proper low frequency cutout filter on the input, these types of filters may overload the active part of filter while trying to compensate the mains voltage [13].

Analyzing the graphs in Figure 17, it can be noticed that type III filters have the biggest insertion loss module. Compared to other filters, this module is much larger and less sensitive to changes both to gain of a filter and impedance module of the receiver (the noise source). Type I filters seem to have the worst parameters, as they have the lowest attenuation and highest sensitivity to changes in the source impedance module.

In the feedforward filters, an important thing is to keep the gain value close to unity. Reducing this to less than unity results in a rapid decrease in the effectiveness of the filter. In contrast, the excess, even slight, can in some cases result in amplification of the noise generated by the receiver, which is obviously not allowed.

5. Summary

First part of this paper carries out a theoretical analysis of the feedback and feedforward active filters. Second part of the article focuses on simulation tests for selected variants of filters presented in the first part. Filters can be divided into six different base types, all of them analyzed in the paper. Parameters such as the insertion loss *IL* and the impedance increase ΔZn have been derived and described. Also, all types of the filters was assessed depending on the nature and type of the noise source.

Eventually, the analyzed types of active filters have been compared in terms of practical applications, on basis of simulation studies. Additionally, possible problems and risks associated with their use have been put under consideration. Conclusions have been drawn, based on the theoretical analysis, literature, and simulation research.

References

[1] Akagi H., Shimizu T.: Attenuation of Conducted EMI Emissions From an Inverter-Driven Motor. IEEE Trans. Power Electron., vol. 23, no. 1, Jan. 2008.

[2] Biela J., Wirthmueller A., Waespe R., Heldwein M. L., Raggl K., Kolar J. W.: Passive and Active Hybrid Integrated EMI Filters. IEEE Trans. Power Electron., vol. 24, no. 5, May 2009.

[3] Boroyevich D., Burgos R.,Arnedo L. Wang F.: Synthesis and integration of future electronic power distribution systems. Proc. IEEE PCC, Nagoya, JP, 2007.

[4] Boroyevich D., Zhang X., Bishinoi H., Burgos R., Mattavelli P., Wang F.: Conducted EMI and Systems Integration. CIPS 2014, Feb., 25-27 2014, Nuremberg/Germany.

[5] Cantillon-Murphy P., Neugebauer T. C., Brasca C., Perreault D. J.: An Active Ripple Filtering for Improving Common-Mode Inductor Performance. IEEE Power Electron. Letters, vol. 2, no. 2, pp.45-50, June 2004.

[6] Chen W., Yang X., Wang Z.: An Active EMI Filtering Technique for Improving Passive Filter Low-Frequency Performance. IEEE Trans. Electromagn. Compat., vol. 48, no. 1, Feb. 2006.

[7] Dong D., Luo F., Zhang D. Boroyevich D., Mattavelli P.: Grid-interface bidirectional converter for residental dc distributions systems - Part 2: AC and dc interface design with passive components minimization. IEEE Trans. Power Electron., vol. 28, no. 4, pp. 1667-1679, Apr. 2013.

[8] Gerber M., Ferreira J. A.: A system integration philosophy for demanding requirements in power electronics. Proc. IEEE IAS, pp. 1389-1396, Sep. 2007.

[9] Heldwein M. L., Ertl H., Biela J., Kolar J. W.: Implementation of a Transformless Common-Mode Active Filter for Offline Converter Systems. IEEE Trans. On Industrial Electron., vol. 57, no. 5, May 2010.

[10] LaWhite L., Schlecht M. F.: Active filters for high frequency power circuits under strict ripple limitations. IEEE PESC Rec., pp. 255, 1986.

[11] LaWhite L., Schlecht M. F.: Design of Active Ripple Filters for Power Circuits Operating in the 1-10 MHz Range. IEEE Trans. Power Electron., vol. 3, no. 3, pp. 310-317, July 1988.

[12] Luo F., Zhang D. Boroyevich D., Mattavelli P., Xue J., Wang F., Gazel N.: On discussion of ac and dc side EMI filters design for conducted noise suppression in dc-feed three-phase motor drive system. Proc. IEEE APEC, Mar. 2011.

[13] Pasko M., Szymczak M.: Porównanie i ocena metod aktywnego tłumienia zaburzeń przewodzonych. IAPGOŚ, vol. 4, no. 4, 2014.

[14] Son Y.-C., Sul S.-K.: Generalization of Active Filters for EMI Reduction and Harmonics Compensation. IEEE Trans. Ind. Appl., vol. 42, no. 2, pp. 545-551, March/April 2006.

[15] Zhang X., Boroyevich D., Mattavelli P., Wang F.: Filter Design Oriented EMI Prediction Model for DC-field Motor Drive System Using Double Fourier Integral Transform Method. Proc. IEEE IPEMC, pp. 1060-1064, 2012.